On how Turbulent Mountain Stress influences sudden stratospheric warming occurrence

Froila M. Palmeiro[1,2], Rolando R. Garcia[3], Natalia Calvo[2] and David Barriopedro[4]
(froila.palmeiro@bsc.es)
[1]Barcelona Supercomputing Center (BSC), Barcelona, Spain
[2] Universidad Complutense de Madrid, Madrid, Spain
[3]National Center for Atmospheric Research (NCAR), Boulder CO, United States
[4]Instituto de Geociencias, IGEO (CESIC-UCM)

Barcelona Supercomputing Center
Centro Nacional de Supercomputación
PRIMAVERA (H2020 GA 641727)
GOBIERNO DE ESPAÑA
MINISTERIO DE CIENCIA, INNOVACIÓN Y UNIVERSIDADES
IGEO INSTITUTO DE GEOCIENCIAS

I. MOTIVATION

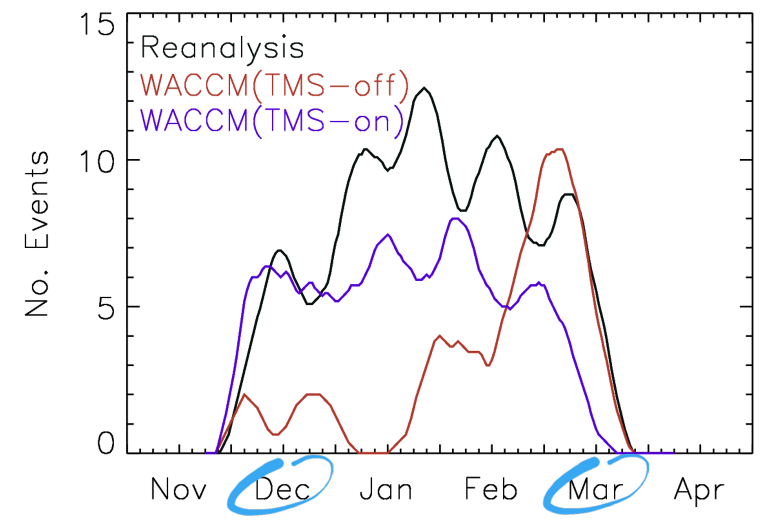

Figure 1: SSW total frequency distribution within ±10-days of the date in the x-axis for 1955 to 2005 derived from NCEP-NCAR reanalysis (black), TMS-on (red) and TMS-off (blue). The frequencies are smoothed with a 10-day running mean. SSWs are defined as zonal-mean zonal wind reversals at 10 hPa in any latitude from 55-70N (Palmeiro et al. 2015)

The implementation of the Turbulent Mountain Stress (TMS) parameterization in the Whole Atmospheric Community Climate Model (WACCM) is critical to obtain a realistic Sudden Stratospheric Warming (SSW) frequency in the Northern Hemisphere (Richter et al. 2010). We found that moreover, the TMS has a critical effect on the intraseasonal occurrence of SSWs: **without TMS most SSWs occur in late winter.**

Comparing two simulations TMS-on and TMS-off in December and March here we elucidate how TMS influences SSW occurrence.

II. MODEL & DATA

MODEL: CESM-WACCM (Community Earth System Model - Whole Atmosphere Community Climate Model) **version 4** (Marsh et al. 2013)

- Longitude x latitude: 2.5˚x 1.9˚ and 66 vertical levels
- *Parameterization of Orographic* gravity waves (McFarlane 1987)
- Turbulent Mountain Stress (TMS) ➡ $\tau = \rho C_d |\vec{V}| \vec{V}$

ρ: density
C_d: drag coefficient depending on not resolved topography
$\vec{V}$: wind vector

DATA: - 2 x 50 yrs TMS-on / TMS-off historical simulations (1955-2005)

- NCEP-NCAR Reanalysis for the same time period

III. RESULTS

A. Surface winds

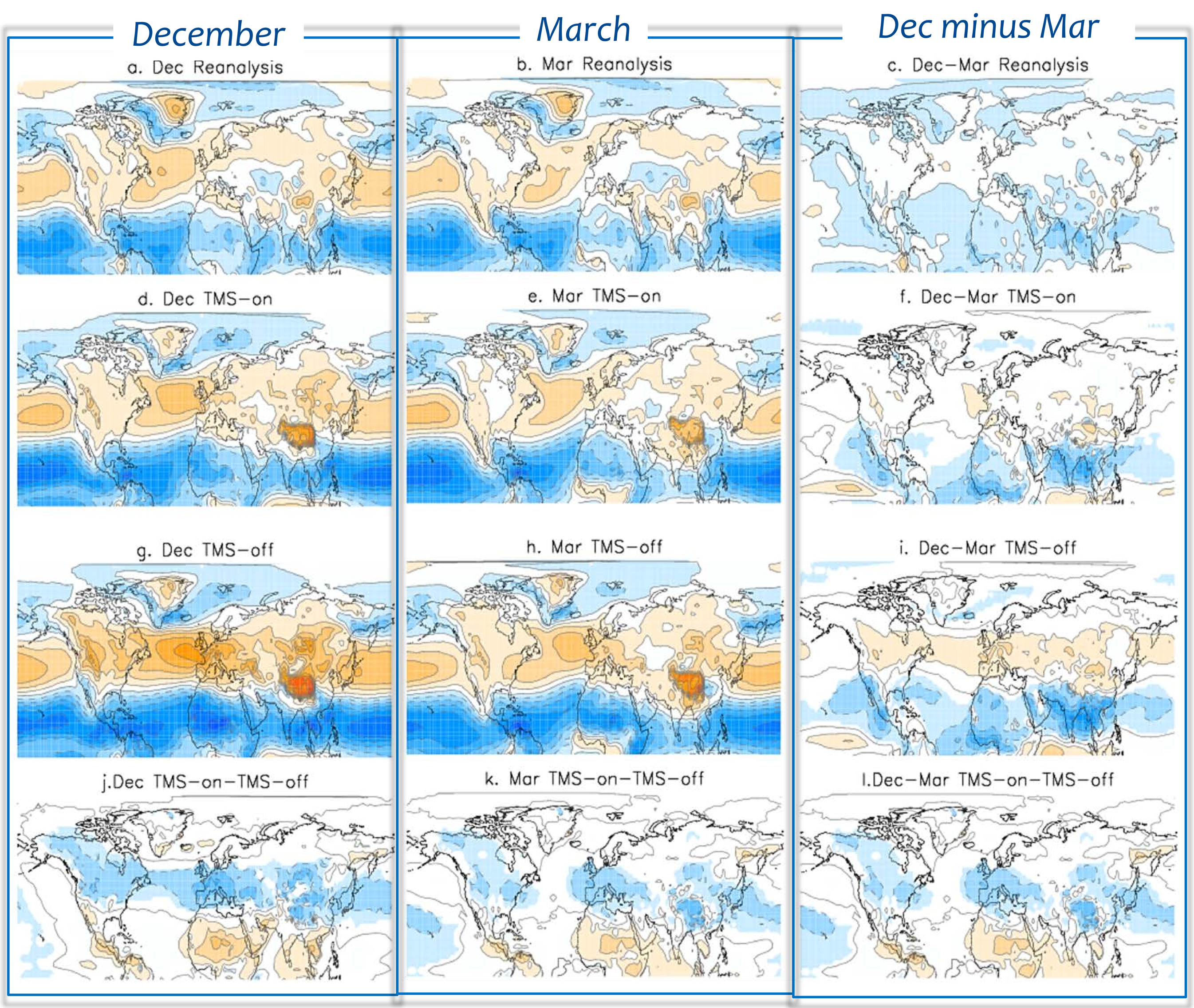

Figure 2: Climatological surface zonal wind (m s^{-1}) in (left column) December, (middle column) March, and (right column) December minus March for: (a-c) NCEP-NCAR reanalysis; (d-f) TMS-on; (g-i) TMS-off; and (j-k) TMS-on minus TMS-off. Contour intervals are every 2 m s^{-1}. Only significant differences at the 95% confidence level are shaded

- Surface wind in **TMS-on is more realistic** than in **TMS-off**, which **overestimates** it **in December**, due to the lack of surface drag.
- **Largest differences** between simulations are downstream of the **regions of high topography**: the Rocky Mountains and the Himalayas.
- **TMS-off** shows a **marked intra-seasonal cycle** in zonal wind, specifically along the belt of westerlies (30-55N, Fig. 3i).
- Similar to reanalysis, TMS-on does not show such an intra-seasonal cycle.

Consistent with the intra-seasonal SSW frequency, TMS-off shows a **marked seasonal cycle** in **surface winds** and **planetary wave propagation** to the upper polar stratosphere. These intra-seasonal differences vanish in TMS-on.

B. Refractive index and EP-Flux vectors

- The minimum $\mathbf{n^2}$ is smaller and **located farther poleward** in **TMS-on** than in TMS-off. This **favors poleward** (equatorward) **propagation** in TMS-on (TMS-off) similar to Richter et al. (2010).
- However, since differences in n^2 **persist the entire winter** (Fig. 4e, f), they are **not sufficient** to explain intraseasonal differences in the SSW frequency.
- EP flux vectors at high latitudes indicate **stronger upward PW propagation in TMS-on** compared to TMS-off in December, but PW propagation **becomes similar in March** due to its increase inTMS-off in that month.

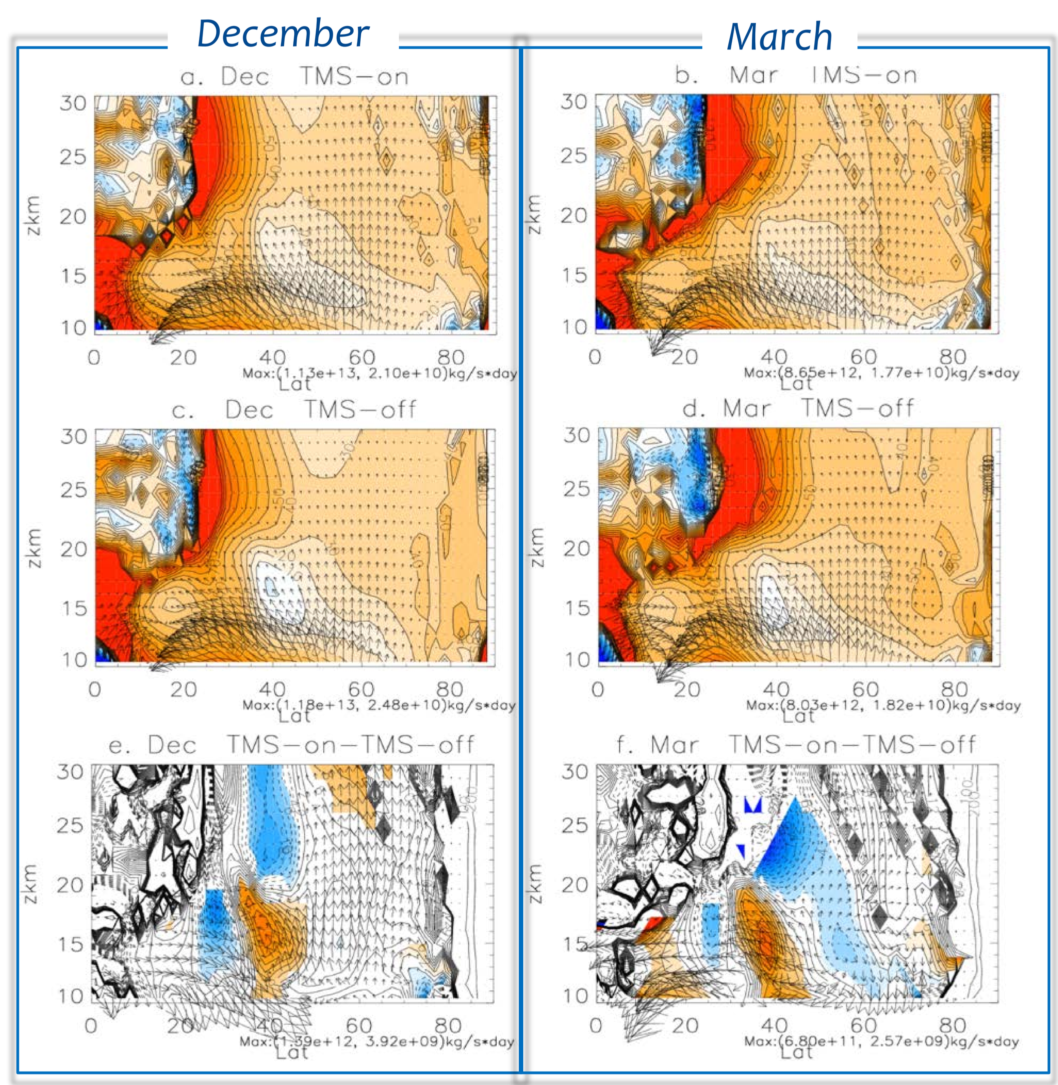

Figure 3. Climatological wave-1 refractive index squared (shaded, dimensionless) and EP flux (vectors, kg s^{-1} day^{-1}) in (left panels) November-December and (right panels) February-March for: (a,b) TMS-on; (d,e) TMS-off; and (c,f) TMS-on minus TMS-off. The refractive index squared has been multiplied by the radius of the earth squared (a^2n^2) so it is dimensionless, and differences are shown in (e,f) only where they are significant at the 95% confidence level. Maximum EP flux values are indicated below each panel. Contour interval is 10 for the climatologies (a-d) and 2 for the differences (e,f).

C. Forcings: EP-flux divergence and Orographic GW drag

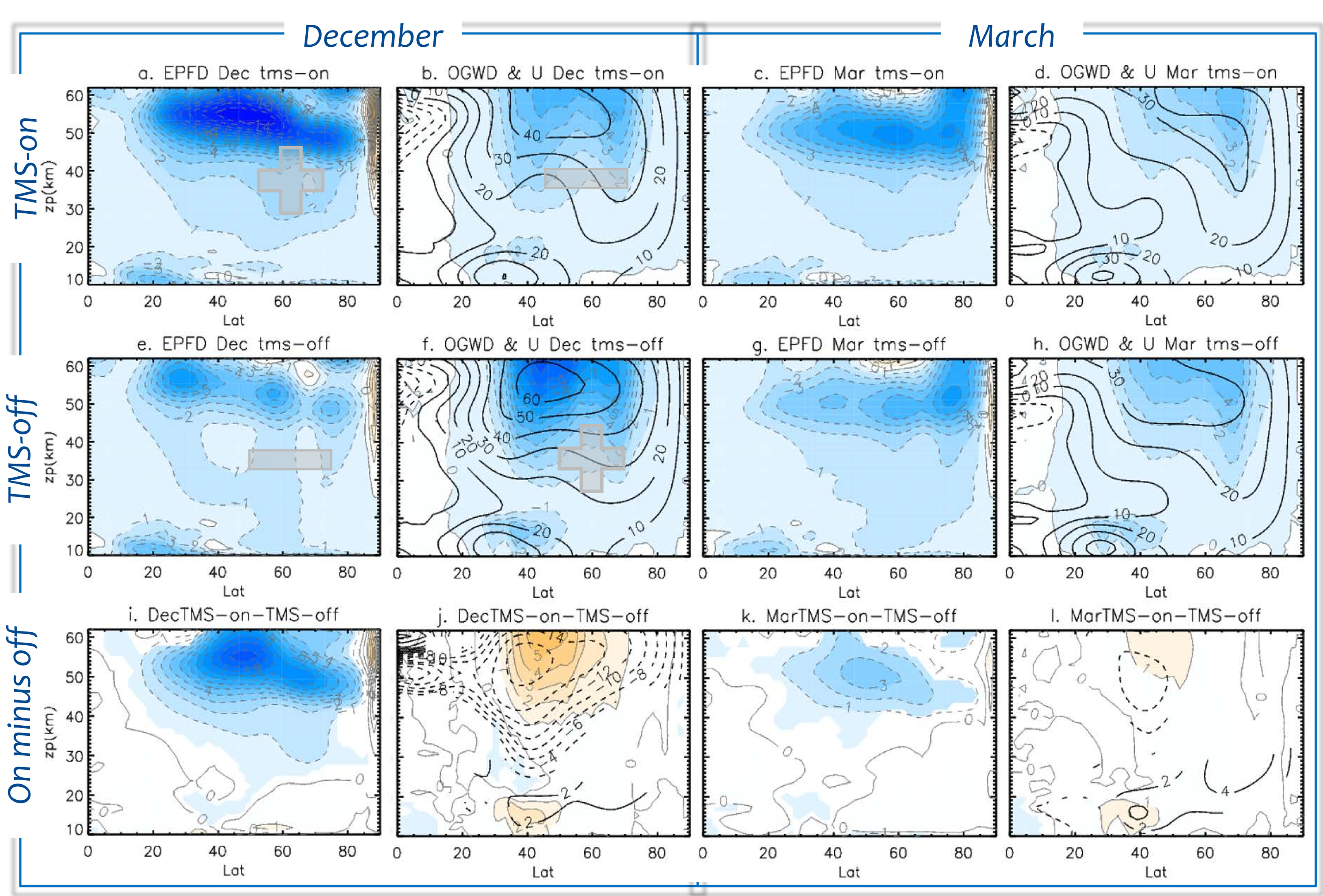

Figure 4. Climatological (first and third column) EP flux divergence (shading, m $s^{-1}day^{-1}$) and (second and fourth column) zonal-mean zonal wind tendency due to OGWD (shading, m $s^{-1}day^{-1}$) in December and March for (top row) TMS-on, (middle row) TMS-off and (bottom row) TMS-on minus TMS-off. For panels showing the zonal-mean zonal wind tendency, black contours denote the zonal-mean zonal wind (m s^{-1}). Contours are every 1 m s^{-1} day^{-1} for the wave forcings and every 10 m s^{-1} (2 m s^{-1}) for the zonal-mean zonal wind climatology (differences). Only significant differences at the 95% confidence level are shown

- In **December**, the **dominant forcing** in **TMS-on** is **the EP flux divergence** (consistent with more SSWs), and the leading driver in TMS-off is the orographic GW drag.
- There is an **apparent compensation between the differences** in EP flux divergence and differences in orographic GW drag, although it is not perfect (cf. Fig. 4i,j).
- In **March**, both **forcings become similar** between simulations (Fig. 4k,l).

Is there a compensation between forcings?

- The hypothesis is that the effective forcing within the region (black box) represents ~75% of the torque due to upward-propagating PW, with this **relative contributions being constant across winter**.
- Since the torque associated with **orographic GW** is **mostly effective in the region** (and GW can only propagate vertically), the effective **planetary wave torque** will be that necessary to **make up the ~75%** expected, with the rest propagating equatorward.
- In **December** the relative contribution to the total torque in **TMS-off** for **OGW is 39%**, so **only 39%** of the torque is associated to **PW**, **versus** the **54% in TMS-on**.

D. Relative contribution of wave momentum fluxes

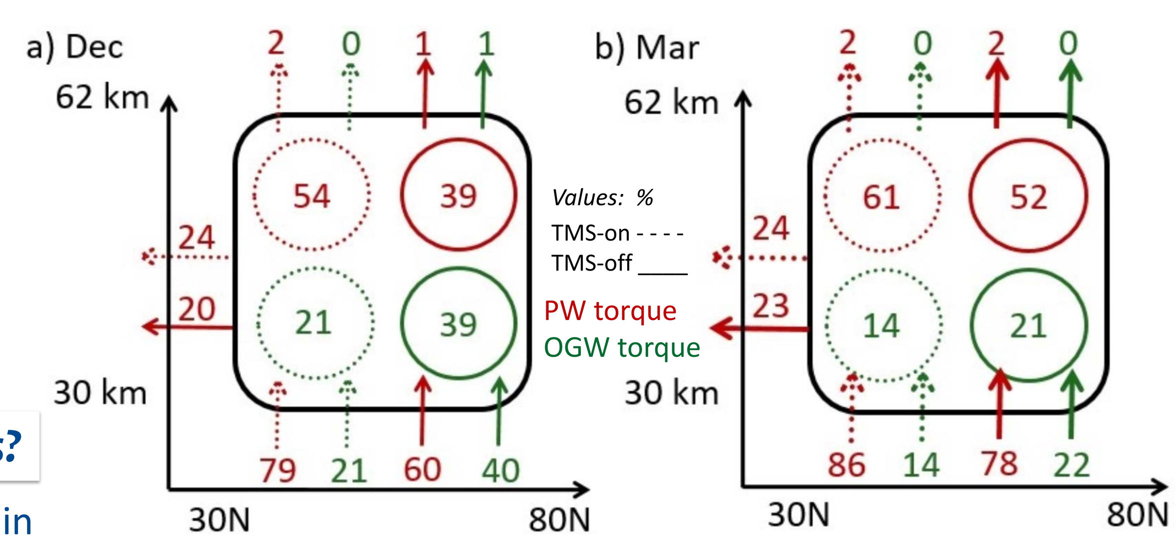

Figure 5: Climatological wave momentum fluxes (arrows) and their associated zonal-mean torques integrated along the boundaries of a region bounded by [30–80]°N and 30-62 km. The numbers next to the dashed (solid) arrow represent the relative contributions of the wave induced torques in the TMS-on (TMS-off) simulation. Numbers in the dashed (solid) circles within each box are the result of evaluating the sum of the wave torques along all boundaries in TMS-on (TMS-off) and characterize the wave forcing in the region denoted by the box. For each simulation and month, torques are expressed as percentages of the total (PW + OGW) torque at the lower boundary (similar to Cohen et al. 2014).

- In contrast, during **March**, the **orographic GW** in **TMS-off torque decreases** to 21%, so the **PW torque increases** to compensate it and becomes similar to the torque in TMS-on.

KEY MESSAGES

- The **TMS** parameterization **weakens surface winds** particularly in regions of high topography (Rocky Mountains and the Himalayan Plateau). This **effect** is **larger in December** so a strong seasonal cycle appears in TMS-off. Weaker surface winds imply **less orographic gravity wave drag** in the stratosphere **in December**.
- We found **a compensation between planetary wave** forcing (associated with SSW occurrence) **and orographic wave** forcing in the extra-tropical stratosphere: when the latter decreases, the planetary waves are refracted farther poleward to compensate so SSWs are more frequent.

References

Cohen, N. Y., E. P. Gerber, and O. Bühler, 2014: What Drives the Brewer–Dobson Circulation? *J. Atmos. Sci.*, **71**, 3837–3855, doi:10.1175/JAS-D-14-0021.1.

Marsh, D. R., M. J. Mills, D. E. Kinnison, J.-F. Lamarque, N. Calvo, and L. M. Polvani, 2013: Climate Change from 1850 to 2005 Simulated in CESM1(WACCM). *J. Clim.*, **26**, 7372–7391, doi:10.1175/JCLI-D-12-00558.1.

McFarlane, N.A., 1987: The effect of orographically excited gravity wave drag on the general circulation of the lower stratosphere and troposphere. J. Atmos. Sci., 44, 1775–1800.

Matsuno, T., 1970: Vertical Propagation of Stationary Planetary Waves in the Winter Northern Hemisphere. *J. Atmos. Sci.*, **27**, 871–883, doi:10.1175/1520-0469(1970)027<0871:VPOSPW>2.0.CO;2.

Palmeiro, F. M., Barriopedro, D., García-Herrera, R. and Calvo, N. (2015). Comparing Sudden Stratospheric Warming Definitions in Reanalysis Data. *Journal of Climate*, 150709110342004. https://doi.org/10.1175/JCLI-D-15-0004.1

Richter, J. H., F. Sassi, and R. R. Garcia, 2010: Toward a Physically Based Gravity Wave Source Parameterization in a General Circulation Model. *J. Atmos. Sci.*, **67**, 136–156, doi:10.1175/2009JAS3112.1.